http://dx.doi.org/10.5012/bkcs.2012.33.5.1777

Assembling Gold Nanocubes Into a Nanoporous Gold Material

Ju-Hwan Oh, Young Jin Sa,[†] Sang Hoon Joo,[†,*] and Jae-Seung Lee[*]

Department of Materials Science and Engineering, Korea University, Seoul 136-713, Korea. [*]E-mail: jslee79@korea.ac.kr
[†]School of Nano-Bioscience and Chemical Engineering, KIER-UNIST Advanced Center for Energy, and Low Dimensional Carbon Materials Center, Ulsan National Institute of Science and Technology (UNIST), Ulsan 689-798, Republic of Korea
[*]E-mail: shjoo@unist.ac.kr
Received October 20, 2011, Accepted February 14, 2012

Key Words : Gold nanocube, Porous material, Assembly, Adsorption isotherm, Dithiothreitol

Nanoporous gold materials (NGM) have been intensively investigated in a variety of areas such as catalysis, energy storage, electrochemistry, and sensing.[1-6] They are also particularly attractive as a platform for observing the critical behavior of liquid helium owing to their unique chemical and physical properties such as high surface area and pore volume.[7,8] The development of NGM synthesis has led to various strategies based upon selective leaching of bimetallic gold alloys,[9] template-based replication,[10] thermal decomposition of gold oxides,[11] thermally and photochemically activated nanoparticle assembly,[12] and electrochemical reactions.[13] These methods, however, require high reaction temperatures, in certain cases even up to 900 ºC, and complicated precedent preparation of alloys or oxides of gold. Moreover, these methods are often followed by post-synthetic thermal annealing to control the pore size, which is not only inconvenient but also time consuming.

Utilizing cubic gold nanostructures with controlled sizes as building blocks for further conceptually complicated nanostructures has been explored in optics, therapeutics, cell imaging, and material synthesis.[14-18] Unlike spherical nanoparticles, these gold nanocubes (AuNCs) exhibit distinctive structural properties such as six identical flat surfaces outlined by twelve sharp edges, which would allow one to build up architectures with substantial diversity in structure. To date, however, only a few types of AuNC assemblies have been reported, most of which are based upon the face-to-face conjunctions induced simply by drying.[19] Such interconnection often results in either a flat tiled surface with uncontrolled defects when assembled two-dimensionally, or bulk superstructures with irregular shapes three-dimensionally, depending upon the assembly reaction conditions. Most of all, these structures are assembled based upon non-covalent secondary bondings, resulting in their instability significantly. Therefore, the synthesis of AuNC-based three-dimensional assemblies with advanced structural properties, in particular associated with porous materials, would be an important progress in materials science.

Herein, we present the synthesis of a NGM by assembling monodisperse AuNCs. We developed a new strategy to assemble the AuNCs *via* conjunctions involving edges and vertices, through which three-dimensionally interconnected nanopores are generated (Scheme 1). The AuNCs are covalently crosslinked by dithiol linkages based on the gold-sulfur chemistry, which provides substantial stability to the NGM. Importantly, this NGM exhibits significantly enlarged surface area and increased pore volume compared to other conventional NGMs, characterized by a nitrogen adsorption and desorption experiment. The NGM is rapidly synthesized at room temperature, excluding any unexpected structural deformation and change in surface properties by elevated temperature treatments.

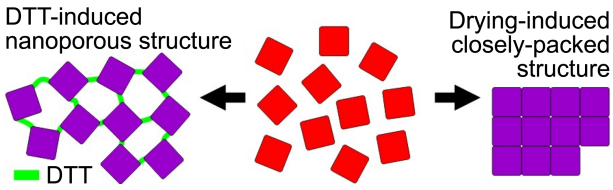

Scheme 1. A scheme illustrating the assembly of gold nanocubes into a DTT-induced nanoporous structure (left) and a closely-packed structure (right).

Before the synthesis of the NGM, we first synthesized the AuNCs using a seed-mediated method for the preparation of the building blocks.[20] The resultant AuNCs exhibited well-defined cubic structures whose average edge length was determined to be 76 nm by transmission electron microscopy (TEM) analysis (Fig. 1(a) and (b)). Subsequently, 0.025 nM of the AuNCs (4 L) were combined with dithiothreitol (DTT) and NaCl for the synthesis of the NGM (final [DTT] and [NaCl] = 10 mM and 0.5 M, respectively). The two terminal thiol groups of DTT play a significant role to covalently bind to the AuNCs. Although the reaction mixture was originally light purple due to the surface plasmon resonance of the nanocubes, it turned dark blue and eventually almost colorless as the reaction proceeded, indicative of the effective macroscopic assembly formation of the AuNCs (Fig. 1(c)). The assembly reaction was further allowed to complete for overnight, leading to the precipitation of the NGM in the form of large aggregates. After the supernatant of the mixture was decanted, the NGM was collected, washed with water three times, and dried under vacuum.

We first investigated the porous structure of the NGM using scanning electron microscopy (SEM). The morphology of the NGM clearly demonstrates that the AuNCs are

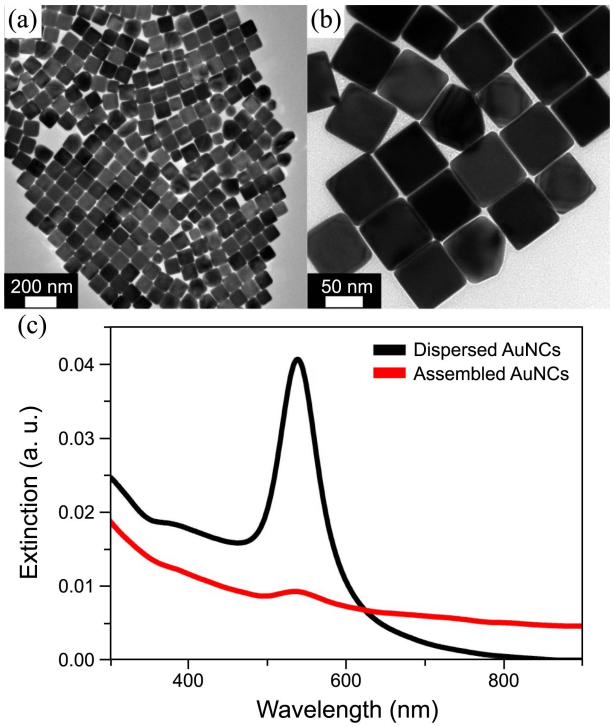

Figure 1. (a) A TEM image of the gold nanocubes synthesized using cetyltrimethylammonium chloride (CTAC) as a structure-directing reagent, and (b) their magnified TEM image. (c) UV-vis spectra of dispersed (black) and assembled (red) gold nanocubes.

assembled *via* the edge-to-edge or vertex-to-edge interactions (Fig. 2(a)), indicating the potential presence of interconnected pores inside of the NGM. In contrast, however, the AuNCs that are assembled simply based upon the drying effect in the absence of DTT resulted in closely-packed superstructures (Fig. 2(b)), as observed in previous literatures.[19] Importantly, the conjunctions of the AuNCs in the NGM predominantly involve the edges and vertices of the cubes, which fundamentally explains the geometric origin for the formation of the pores. In fact, any face-to-face interactions of the AuNCs would have resulted in the densely packed structures only, leading to little space and thus negligible pores between the cubes. We attribute the selective formation

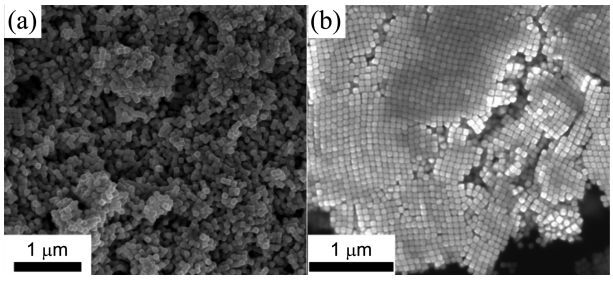

Figure 2. (a) An SEM image of the nanoporous gold material (NGM) synthesized using DTT as a crosslinker of AuNCs. Note that the morphology of the NGM exhibits a number of nanopores. (b) An SEM image of the closely-packed structure of AuNCs induced by the drying effect. Nanopores are hardly observed, while only a few macroscopic cracks between the large AuNC assembly domains sparsely exist.

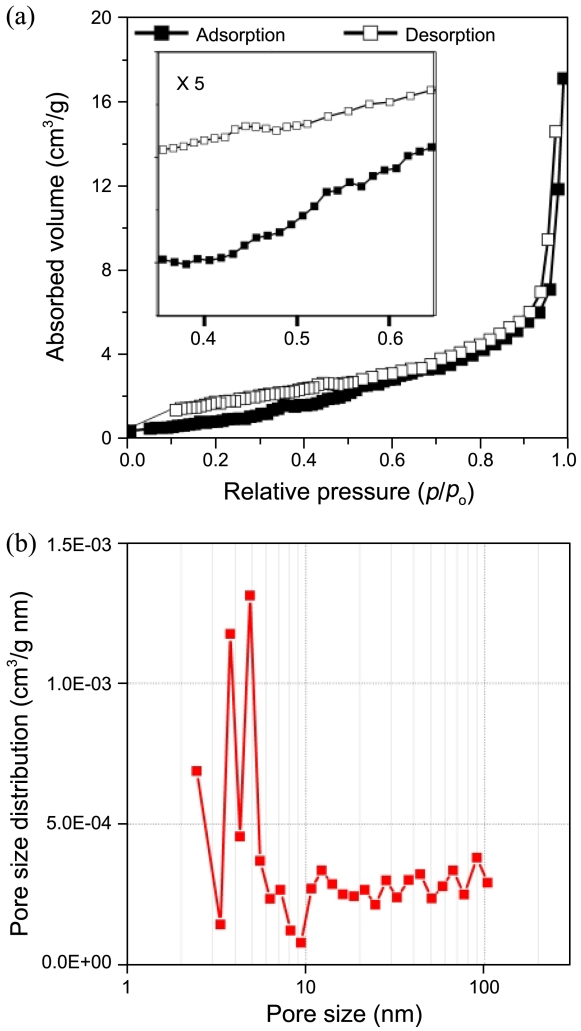

Figure 3. (a) Isotherm of N_2 adsorption-desorption of the NGM measured at −196 °C. Note that a common hysteresis and increase in adsorption is observed from P/P_o = 0.4 to 0.6 in the magnified curve (inset), indicating that the NGM is mesoporous. (b) Pore size distribution of the NGM calculated by BJH method. Note that the distribution is almost monodisperse, indicating the pore size of the NGM is nearly even and consistent in the entire structure.

of the assemblies that involve edges and vertices of the AuNCs to the preferential binding of DTT to the edges or vertices of the AuNCs.[21] In fact, the curvature of gold nanomaterials are known to play a significant role in selectively and thermodynamically providing the priority for their interactions with thiols to the surfaces with higher curvatures such as edges and vertices of the AuNCs.[21] The presence of polythiol crosslinkers, therefore, would be crucial for the formation of the NGM.

We further characterized the pore structures by measuring the isotherm of N_2 adsorption and desorption at −196 °C (Belsorp-Max, BEL) after vacuum-drying at 100 °C for 12 hours. As expected, we observed a characteristic, yet somewhat weak hysteresis loop that are associated with the presence of nanopores inside of the NGM (Fig. 3(a)). The dramatic increase and decrease took place at relatively higher nitrogen pressure (P/P_o = ~0.9), potentially indicating

the presence of considerable portion of macropores (pore size = 50-100 nm) between large AuNC aggregate domains. These macropores can be also identified by SEM (Fig. 2(a)). In addition, we analyzed the pore size distribution using the Barrett-Joyner-Halenda (BJH) method for pores below 100 nm, and obtained the maximum peak intensity at 4.85 nm in size (Fig. 3(b)). The abundance of the peaks below 10 nm in size indicates the high portion of mesopores in the NGM synthesized in this work, which is consistent with the increase in adsorption at P/P_o = 0.4-0.6 (Fig. 3(a), inset). Importantly, the presence of both macropores and mesopores in the NGM makes the material exceptionally attractive as a hierarchical dual pore system. The total pore volume and the Brunauer-Emmett-Teller (BET) surface area were determined to be 3.37×10^{-2} cm^3/g and 4.7 m^2/g, respectively. The surface area of the NGM is considerably increased compared to conventional metallic nanoporous materials (typically 0.5 m^2/g)[8]. To the best of our knowledge, this work is one of only a few examples of investigations for the pore structures using the N_2 isotherm measurement, which provides highly convincing and accurate analysis of the three-dimensionally interconnected pores compared to other observations that depend on only electron microscopy. While disordered, the isotropic geometry of the pore would provide isotropic properties to the NGM, which is specifically attractive to chemical applications such as catalysis and superstructured templates.

We finally investigated how the size of the AuNC affected the assembly and pore structure. Smaller AuNCs (edge length = 45 nm) were synthesized (Fig. 4(a)) using the similar method except the higher concentration of the seeds (2.6 times higher than larger AuNCs), and assembled using DTT in the presence of NaCl in the similar manner for the NGM. To our surprise, we only obtained the closely but disorderly packed assembly structure of the smaller AuNCs, where we hardly observed porous structures (Fig. 4(b)). The closely-packed structures *via* face-to-face interactions of the smaller AuNCs could be explained by their decreased size and thus relatively increased surface potential, leading to enhanced face-to-face interactions. The more truncated edges and vertices of the smaller AuNCs also contributed to the formation of non-porous structures because of the decreased curvature, analogous to the assembly of spherical particles.

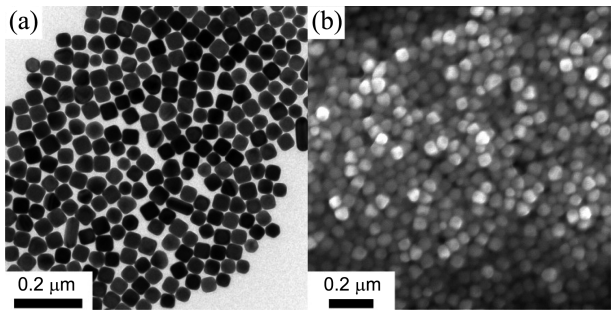

Figure 4. (a) A TEM image of smaller AuNCs (edge length = 45 nm), and (b) an SEM image of the assembled smaller AuNCs using DTT as a crosslinker of AuNCs. Note that the smaller AuNCs assembled in a closely-packed, yet disordered way with negligible local porous structures.

In conclusion, we have synthesized a new NGM by covalently assembling cubic gold structures based on their site-specific thiol reactivity. This NGM has distinctive mesopores whose pore volume and pore surface area are accurately characterized by measuring an N_2 isotherm. We have also demonstrated that the size and shape of the AuNC as a building block play a significant role in determining the morphology and porosity of the assembled structure. Importantly, this study is a significant advance that shows how the result of a bottom-up approach could be affected by the properties of its unit building block, illustrating the importance of regulating the fundamental properties of nanomaterials for their assembly structures. Based on this work, one can expect further advanced NGMs whose pore structure is spatially ordered by modulating the facet-specific interactions of more complicated and well defined nanoparticles, or whose pore size is systematically controlled by employing crosslinkers with various lengths.

Experimental

Cetyltrimethylammonium chloride (CTAC, Cat. # H0082) was purchased from Tokyo Chemical Industry Company (TCI, Tokyo, Japan). Dithiothreitol (DTT, Cat. # 43815), gold chloride trihydrate (Cat. # 520918), L-ascorbic acid (Cat. # A5960), sodium borohydride (Cat. # 480886), sodium bromide (Cat. # S4547), sodium chloride (Cat. # S7653) and other chemicals were purchased from Sigma-Aldrich (Milwaukee, WI, USA) and used without further purification.

Gold nanocubes (AuNCs) were prepared by the seed-mediated growth method that is previously reported in Reference 20. In brief, gold nanoparticle seeds were prepared by reducing 10 mL of 0.25 mM $HAuCl_4$ solution containing 0.1 M CTAC with 0.45 mL of 0.02 M ice-cold $NaBH_4$ while stirring vigorously. The resulting solution immediately turned brown and was incubated for 1 hour at 30 °C. Subsequently, two growth solutions, each composed of 0.25 mL of 10 mM $HAuCl_4$, 0.01 mL of 10 mM NaBr, 0.09 mL of 40 mM ascorbic acid, 2 mL of 0.5 M CTAC and 7.625 mL of deionized water, were prepared and kept in a water bath at 30 °C. Next, 0.025 mL of the seed solution was added to one of the growth solutions with gentle shaking until the solution color turned light pink (~5 sec). Then 0.025 mL of the mixture was immediately added to the other growth solution with gentle shaking for ~10 sec. The final mixture was left undisturbed for 15 min for particle growth. The NGM was prepared by addition of 116.9 g of NaCl and 6.17 g of DTT to 4 L of 0.025 nM AuNC solution while stirring vigorously (final [DTT] and [NaCl] = 10 mM, and 0.5 M, respectively). The color of the mixture changed from light purple to almost colorless indicating the macroscopic assembly formation. The mixture was left undisturbed for 12 hours to complete the assembly formation.

The UV-vis absorption spectra of the AuNCs and NGMs were characterized by using Agilent 8453 UV-vis spectro-

photometer equipped with a Peltier temperature controller. The controlled sizes and shapes of both materials characterized by using filed emission scanning electron microscopy (FE-SEM Hitachi S-4800) and transmission electron microscopy (TEM, TECNAI-20). The porous structure of the NGMs was analyzed by an N_2 adsorption experiment at −196 ºC using a BEL Belsorp-Max machine. The surface area and pore size distribution of the NGMs were calculated by using the Brunauer-Emmett-Teller (BET) equation and the Barrett-Joyner-Halenda (BJH) method, respectively.

Acknowledgments. This work was supported by the 2nd stage of the Brain Korea 21 Project in 2012, Basic Science Research Program through the National Research Foundation of Korea (NRF) funded by the Ministry of Education, Science and Technology (Grant No. 2011-0027400 and 2011-0005713), and the TJ Park Junior Faculty Fellowship.

References

1. Biener, M. M.; Biener, J.; Wichmann, A.; Wittstock, A.; Baumann, T. F.; Baumer, M.; Hamza, A. V. *Nano Lett.* **2011**, *11*, 3085.
2. Stevens, G. B.; Reda, T.; Raguse, B. *J. Electroanal. Chem.* **2002**, *526*, 125.
3. Jin, X.; Zhuang, L.; Lu, J. *J. Electroanal. Chem.* **2002**, *519*, 137.
4. Bonroy, K.; Friedt, J.-M.; Frederix, F.; Laureyn, W.; Langerock, S.; Campitelli, A.; Sara, M.; Borghs, G.; Goddeeris, B.; Declerck, P. *Anal. Chem.* **2004**, *76*, 4299.
5. Noort, D.; Rani, R.; Mandenius, C.-F. *Microchim. Acta* **2001**, *136*, 49.
6. Wang, X.-Y.; Zhong, H.; Lv, Y.; Chen, H.-Y. *Chem. Lett.* **2003**, *32*, 1054.
7. Csathy, G. A.; Tulimieri, D.; Yoon, J.; Chan, M. H. W. *Phys. Rev. Lett.* **1998**, *80*, 4482.
8. Walsh, D.; Arcelli, L.; Ikoma, T.; Tanaka, J.; Mann, S. *Nat. Mater.* **2003**, *2*, 386.
9. Erlebacher, J.; Aziz, M. J.; Karma, A.; Dimitrov, N.; Sieradzki, K. *Nature* **2001**, *410*, 450.
10. Attard, G. S.; Bartlett, P. N.; Coleman, N. R. B.; Elliott, J. M.; Owen, J. R.; Wang, J. H. *Science* **1997**, *278*, 838.
11. Jurczakowski, R.; Hitz, C.; Lasia, A. *J. Electroanal. Chem.* **2004**, *572*, 355.
12. Kim, M.; Jeong, G. H.; Lee, K. Y.; Kwon, K.; Han, S. W. *J. Mater. Chem.* **2008**, *18*, 2208.
13. Hoogvliet, J. C.; Dijksma, M.; Kamp, B.; van Bennekom, W. P. *Anal. Chem.* **2000**, *72*, 2016.
14. Chen, H.; Sun, Z.; Ni, W.; Woo, K. C.; Lin, H.-Q.; Sun, L.; Yan, C.; Wang, J. *Small* **2009**, *5*, 2111.
15. Wu, X.; Ming, T.; Wang, X.; Wang, P.; Wang, J.; Chen, J. *ACS Nano* **2010**, *4*, 113.
16. Skrabalak, S. E.; Chen, J.; Sun, Y.; Lu, X.; Au, L.; Cobley, C. M.; Xia, Y. *Accounts Chem. Res.* **2008**, *41*, 1587.
17. Murphy, C. J. *Science* **2002**, *298*, 2139.
18. Zhang, J.; Langille, M. R.; Personick, M. L.; Zhang, K.; Li, S.; Mirkin, C. A. *J. Am. Chem. Soc.* **2010**, *132*, 14012.
19. Ren, J.; Tilley, R. D. *J. Am. Chem. Soc.* **2007**, *129*, 3287.
20. Wu, H. L.; Kuo, C. H.; Huang, M. H. *Langmuir* **2010**, *26*, 12307.
21. Kou, X.; Sun, Z.; Yang, Z.; Chen, H.; Wang, J. *Langmuir* **2009**, *25*, 1692.